

Journal of Materials Chemistry B

Accepted Manuscript



This is an *Accepted Manuscript*, which has been through the Royal Society of Chemistry peer review process and has been accepted for publication.

Accepted Manuscripts are published online shortly after acceptance, before technical editing, formatting and proof reading. Using this free service, authors can make their results available to the community, in citable form, before we publish the edited article. We will replace this *Accepted Manuscript* with the edited and formatted *Advance Article* as soon as it is available.

You can find more information about *Accepted Manuscripts* in the [Information for Authors](#).

Please note that technical editing may introduce minor changes to the text and/or graphics, which may alter content. The journal's standard [Terms & Conditions](#) and the [Ethical guidelines](#) still apply. In no event shall the Royal Society of Chemistry be held responsible for any errors or omissions in this *Accepted Manuscript* or any consequences arising from the use of any information it contains.

Controllable drug release and effective intracellular accumulation highlighted by anisotropic biodegradable PLGE nanoparticles

Cite this: DOI: 10.1039/x0xx00000x

Received 00th January 2013,
Accepted 00th January 2013

Jun-Bing Fan,^{a,c} Yongyang Song,^{a,c} Hongfu Li,^a Jin-Peng Jia,^b Xinglin Guo*,^a and Lei Jiang^a

DOI: 10.1039/x0xx00000x

www.rsc.org/

Control of stretching or compressing ratio of spherical nanoparticles (NPs) leads to a dramatic change in shape and size for particles based on amphiphilic biodegradable poly(lactide-co-glycolide-*b*-ethylene glycol-*b*-lactide-co-glycolide) (PLGE) triblock copolymers. The drug release, endocytosis and intracellular accumulation test of anisotropic PLGE NPs show significantly enhanced properties in comparison with spherical NPs, indicating they are good candidates for drug delivery.

The continuing interest in colloidal polymer NPs, poses questions toward their special properties, such as shape or surface chemistry, which would eventually lead to special applications in healthcare fields.¹⁻⁴ Theoretical calculation and fundamental research indicate that colloidal NPs with anisotropic shape or surface chemistry have superiorities over spherical particles.⁵ It has been found that filomicelles can significantly enhance the circulation time in blood up to ten times as spherical micelles.⁶ During transportation and circulation process *in vivo*, the endocytosis and intracellular distribution of particles are strongly depended on their anisotropic shapes.⁷⁻⁹ Various approaches have been developed for the controlled synthesis of anisotropic micro/nano particles in recent years, such as lithography,¹⁰ freezing,¹¹ microfluidics,^{12,13} self-assembly,^{14,15} swelling of spherical particles,¹⁶ and nonwetting template molding¹⁷. Although these approaches successfully synthesize various anisotropic particles including ring, triangle, cylinder, cuboid, hole-shell, rod, disk, ellipsoid, sphere aggregate cluster, cavity, dumbbell, and crescent moon, their problems remain in terms of high cost, limited particle size, or low yield.¹⁸ Recently, the film stretching method has been reported as a facile, versatile, inexpensive and high throughput method to fabricate polymer anisotropic micro/nano particles.^{1,9,18-21}

However, the most of the anisotropic particles synthesized by film stretching are hydrophobic, or some of them are toxic and non-biocompatible, usually based on the polystyrene.^{9,18,20} There are few researches focusing on the synthesis of anisotropic NPs with amphiphilic, biodegradable and biocompatible properties. Actually, amphiphilic copolymer NPs as novel carrier not only can realize high drug loading capacity, but also exhibit unique disposition characteristics in the body.^{22,23} Therefore, it is very meaningful to

synthesize polymer NPs carriers which possess amphiphilic, biocompatible and biodegradable properties. PLGE has been considered as a very popular biodegradable and biocompatible triblock copolymer used for drug delivery vehicles. It has been proved that the biocompatibility of delivery vehicles would be greatly improved by incorporation of hydrophilic poly(ethylene glycol) (PEG) segment into hydrophobic polymer chain. Meanwhile, owing to the immiscibility between PEG and PLGA (poly(lactic-co-glycolide)), hydrophilic PEG in copolymer would greatly affect the morphology of micro/nano structures during the self-assembly process.²³⁻²⁵ These morphologies of particles combining with their unique properties will potentially improve their drug release, *in vivo* transportation, circulation, targeting, endocytosis and adhesion behavior on vascular wall.^{1,5,6,8} Taking the morphology and biocompatibility of polymer particles into consideration, it is very urgent to synthesize anisotropic drug-loaded PLGE NPs and to use them in the healthcare fields.

In this paper, a series of anisotropic amphiphilic biocompatible and biodegradable PLGE NPs with tunable length/width aspect ratio (AR) can be synthesized from spherical PLGE NPs by a simple film stretching/compressing method. The anisotropic morphologies include ellipsoids, rods, spherical and elliptical disks. The drug release behavior and endocytosis of Nile red (NR) loaded PLGE NPs have also been discussed in detail.

The synthesis of PLGE triblock copolymer was described in our previous work,²⁵ and the detailed characterization of PLGE copolymer was presented in Table S1. By an emulsification-diffusion method (ESI), we synthesized three spherical PLGE NPs with different sizes, including 126 ± 34 nm (sphere1), 75 ± 16 nm (sphere2) and 69 ± 12 nm (sphere3) (Fig. S1). These spheres were used for subsequent film stretching/compressing procedure.

Fig. 1A described the scheme diagram of the synthesis route from spherical to anisotropic NPs by hot stretching, cold stretching and hot compressing. Hot stretching meant stretching after heating, cold stretching meant stretching before heating, and hot compressing meant compressing after heating. In a typical process of hot-stretching, 10% w/v PVA and 2% v/v glycerol were added to the concentrated suspension of spherical PLGE NPs. The mixture was poured into a horizontal groove and casted into an even film till homogeneous. After the film was dried at room temperature, it was cut into sections of ca. 1.5 cm × 6 cm and fixed on a homemade apparatus. After being heated under 90 °C for 15 min, the film was

stretched by 60% or 120% and kept at the temperature for another 15 min. Finally, the film was quickly cooled by liquid nitrogen. After the films gradually recovered to room temperature, they were immersed in water to redissolve PVA under magnetic stirring. The anisotropic PLGE NPs were separated from the solution, washed by water for three times, and freeze-dried for 48 h.

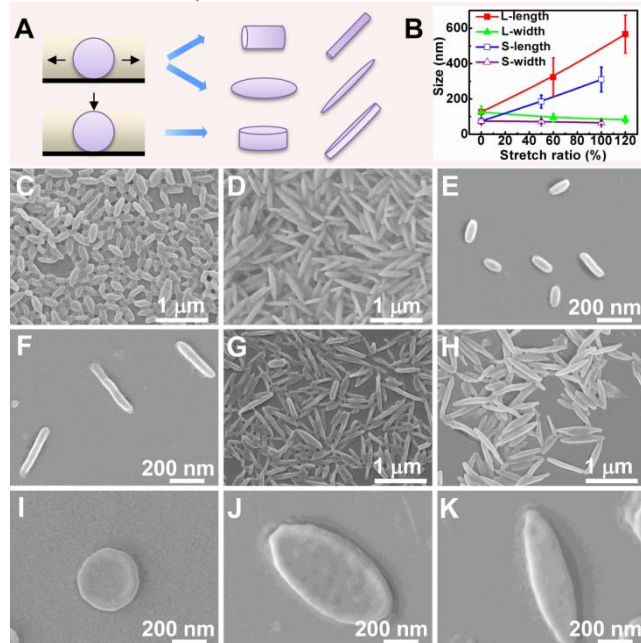


Fig. 1 Anisotropic PLGE NPs fabricated from spherical NPs by hot stretching, cold stretching and hot-compressing. (A) A scheme diagram describing the film stretching/compressing method for fabricating anisotropic NPs. (B) Relationship between stretch ratio and size of anisotropic NPs. L represents large spheres, and S represents small spheres. The relationship between stretch ratio($x\%$) and size(y/nm) of anisotropic NPs can be formulated as follows: L-length, $y = 3.67x+118$; L-width, $y = -0.358x+122$; S-length, $y = 2.35x+72.5$; S-width, $y = -0.1x+75.7$. (C-D) Nanoellipsoids, cold stretching, 100%, 200%; (E-H) nanorods, hot stretching, 60%, 120%, 120%, 150%; (I-K) Nanodisks, hot-compressing, 200%, 200%, 100%.

Table 1 Characters of different NR loaded PLGE NPs. Rod1, rod2 and disk represent NPs stretched by 60%, 120% and compressed by 130% from the sphere, respectively.

Morphology	Length (nm)	Width (nm)	AR	Yield (%)	DL (%)	EE (%)
Sphere	128 ± 35	128 ± 35	1.0 ± 0.0	73.3	1.16	85.0
Rod1	366 ± 77	103 ± 17	3.6 ± 0.9	66.4	1.15	76.4
Rod2	523 ± 141	82 ± 15	6.6 ± 2.0	65.9	1.14	75.1
Disk	313 ± 66	313 ± 66	1.0 ± 0.0	71.8	1.08	77.5

By stretching/compressing different sizes of spherical NPs, a series of anisotropic NPs were obtained, and representative scanning electron microscope (SEM) images were given in Fig. 1C-K. Nanoellipsoids (Fig. 1C-D) were obtained by cold stretching when the stretching ratio was 100% and 200% (from sphere1), respectively. Nanorods (Fig. 1E-H) were obtained by hot stretching when the stretching ratio was 60%, 120% (from sphere3), 120%, and 150% (from sphere2), respectively. Circular disks (Fig. 1I) and elliptical nanodisks (Fig. 1J-K) were obtained by hot-compressing when the stretching ratio was 200% (from sphere2), 200%, and 100% (from sphere1), respectively. It could be concluded that the stretching procedure tended to fabricate nanorods or nanoellipsoids, while compressing method tended to fabricate nanodisks. Therefore, the

morphology of anisotropic NPs could be well controlled by this simple film stretching/compressing method. Additionally, the relationship between stretching ratio and the size of the NPs could be obtained by measuring the length and width of the NPs. As shown in Fig. 1B, the length of nanoparticles increased linearly with increasing the stretching ratio, while the width decreased linearly with increasing the stretching ratio. In detail, when large spherical nanoparticles with diameter of 126 ± 34 nm were stretched by 60%, the length increased to 323 ± 109 nm, while the width decreased to 94 ± 23 nm. When they were stretched by 120%, the length increased to 566 ± 107 nm, while the width decreased to 83 ± 17 nm. The relationship between stretch ratio($x\%$) and size(y/nm) of anisotropic NPs can be formulated as follows: L-length, $y = 3.67x+118$; L-width, $y = -0.358x+122$; S-length, $y = 2.35x+72.5$; S-width, $y = -0.1x+75.7$. The results indicated that the morphology and size of anisotropic NPs could be reasonably tuned by controlling the stretching/compressing ratio.

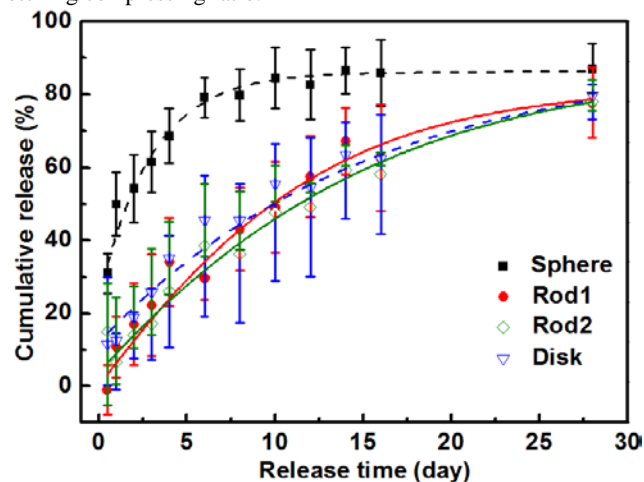


Fig. 2 Morphology mediated drug release behavior of NR loaded PLGE NPs at different time. Spherical NPs displayed a burst release phenomenon, while the anisotropic NPs showed a sustained release.

Four kinds of NR loaded PLGE NPs, namely sphere, rod1, rod2, and disk were chosen to investigate their drug encapsulation and release behavior. As shown in Table 1, PLGE NPs with different morphologies had a similar drug loading (DL) of 1.1% and drug encapsulation efficiency (EE) of about 80%. As shown in Fig. 2, the cumulative release of spherical NPs had already reached 50% at the first day, however, the anisotropic NPs demonstrated much lower drug release, only 11% for rod1, 7% for rod2 and 12% for disk. When the time was increased to the 6th day, the cumulative release of spherical NPs reached up to 79%, and there was no obvious increase in the subsequent time. Meanwhile, it was found that drug-loaded anisotropic PLGE NPs show a similar drug release tendency. Compared to rods, drug-loaded disks exhibit slightly faster than rods. Moreover, drug-loaded rod2 nanoparticles with longer length and narrower width exhibited more sustained drug release than rod1 and disks. The results revealed that drug loaded spherical NPs presented a serious burst release phenomenon at the initial stage and the release rate gradually slowed down after 6 days. However, the cumulative releases of rod1, rod2 and the disk remained very active, which rose at a consistent rate to the 28th day, demonstrating a sustained release. The burst release may be related to the drug adsorbed on the particle surface.^{26, 27} By calculating the volume of the NPs (Fig. S3 and Cal. S1) when the particles were supposed to be uniform (Fig. S2), it was convenient to find that the stretched NPs had a higher volume (3.05×10^6 nm³/particle for rod1, and 2.76×10^6 nm³/particle for rod2) than spheres (1.10×10^6 nm³/particle). Because the higher volume of anisotropic NPs, the drug content on

the surface of spherical NPs should be higher than that of rods at the similar drug encapsulation efficiency. Therefore, we inferred that the difference between burst release of spherical NPs and sustained release of anisotropic NPs could be owed to the morphology.

Endocytosis experiment was also been conducted in vitro to test the interactions between NPs and cells. The results of MCF-7 endocytosis experiment were shown in Fig. 3. It was observed that both spherical and rod shaped PLGE nanoparticles exhibited perinuclear accumulation. However, it should be noted that cells with engulfed rods had stronger fluorescence brightness than cells with engulfed spherical NPs (Fig. 3G). The result suggested that morphology had an important influence on the interaction between cells and drug-loaded NPs. The enhancement of endocytosis from spherical to anisotropic NPs was mainly induced by the adhesion ability, which determined their interactions with cells. The adhesion ability strongly depended on the particle morphology and surface chemistry.^{1, 5} We calculated the surface area of sphere, rod1, and rod2. The results shown in Cal. S1 demonstrated that there was an increment of the surface area from spherical NPs ($5.14 \times 10^4 \text{ nm}^2/\text{particle}$) to anisotropic NPs ($1.35 \times 10^5 \text{ nm}^2/\text{particle}$ for rod1, and $1.45 \times 10^5 \text{ nm}^2/\text{particle}$ for rod2). Therefore, The anisotropic NPs with same surface area as spheres had stronger adhesion abilities, which should be attributed to the enhanced adhesion area. Our results revealed that the surface area of the rods was much larger than that of the spherical NPs, which may lead to an enhanced interaction between NPs and cells, thus to result in the enhancement of endocytosis.

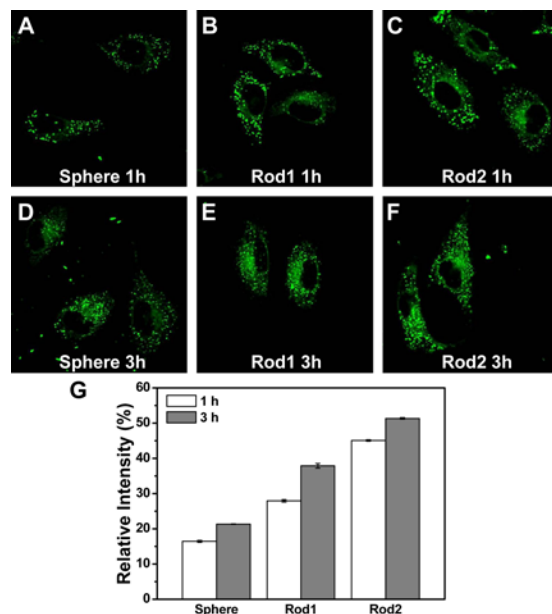


Fig. 3 Morphology triggered endocytosis enhancement of anisotropic NPs. (A) Sphere for 1h, (B) rod1 for 1h, (C) rod2 for 1h, (D) sphere for 3h, (E) rod1 for 3h, (F) rod2 for 3h, and (G) the fluorescence intensity analysis of endocytosed nanoparticles with different time.

To investigate the morphology stability of anisotropic NPs at body temperature, we dispersed and shook PLGE nanorods in 37 °C and 50 °C water bath for 10 min, respectively. SEM images (Fig. 4) of initial and thermal treated nanorods illustrated that there was no morphology change after thermal treatment at 37 °C, while there was an obvious decrease of AR from 6.9 to 4.7 at 50 °C. The change was not obvious when the rods were treated in PBS (phosphate buffer saline) solution or for 12 h (Fig. S4) at 37 °C. This phenomenon maybe induced by phase transition when the thermal treatment

temperature was above T_g of PLGE.²³ The results indicated that the morphology of the synthesized anisotropic PLGE NPs was stable enough when they were circulating in the body.

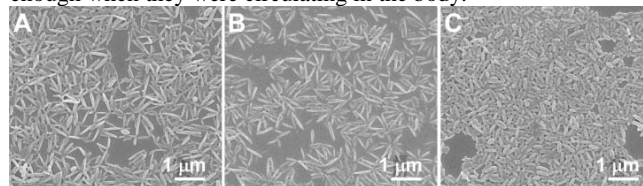


Fig. 4 Morphology stability of anisotropic PLGE NPs. Nanorods (A) without thermal treatment, treated at (B) 37 °C, and (C) 50 °C for 10 min. There was no morphology change at 37 °C, while the AR changed from 6.9 to 4.7 at 50 °C.

In conclusion, we synthesized various anisotropic PLGE NPs with controllable size and morphology by the film stretching/compressing method. The drug release and endocytosis of anisotropic PLGE NPs showed significantly enhanced properties than spherical NPs. The morphology of the synthesized anisotropic PLGE NPs was stable enough when they were treated at body temperature, indicating they are promising candidates for drug delivery.

This research is supported by the National Natural Science Foundation of China (51073165).

Notes and references

^a Beijing National Laboratory for Molecular Sciences (BNLMS), Key Laboratory of Organic Solids, Institute of Chemistry, Chinese Academy of Sciences, Beijing 100190, P. R. China; ^b Department of Orthopedics, General Hospital of Chinese PLA, Beijing 100853, China; ^c These authors contributed equally to the practical work.

Email: xlguo@iccas.ac.cn ; Tel: +86-010-82621396

Fax: +86-010-82627566

† Electronic Supplementary Information (ESI) available: Synthesis of PLGE, PLGE NPs, NR loaded PLGE NPs, drug encapsulation, release, and endocytosis, characterization of PLGE copolymer, calculation of particle surface and volume, and other materials. See DOI: 10.1039/c000000x/

- J. A. Champion, Y. K. Katare and S. Mitragotri, *J. Controlled Release*, 2007, 121, 3-9.
- A. M. Smith and S. Nie, *Acc. Chem. Res.*, 2009, 43, 190-200.
- Z.-Y. Qiao, R. Ji, X.-N. Huang, F.-S. Du, R. Zhang, D.-H. Liang and Z.-C. Li, *Biomacromolecules*, 2013, 14, 1555-1563.
- J.-B. Fan, C. Huang, L. Jiang and S. Wang, *J. Mater. Chem. B*, 2013, 1, 2222-2235.
- P. Decuzzi and M. Ferrari, *Biomaterials*, 2006, 27, 5307-5314.
- Y. Geng, P. Dalhaimer, S. Cai, R. Tsai, M. Tewari, T. Minko and D. E. Discher, *Nat. Nanotech.*, 2007, 2, 249-255.
- B. D. Chithrani, A. A. Ghazani and W. C. Chan, *Nano Lett.*, 2006, 6, 662-668.
- S. E. Gratton, P. A. Ropp, P. D. Pohlhaus, J. C. Luft, V. J. Madden, M. E. Napier and J. M. DeSimone, *Proc. Natl. Acad. Sci.*, 2008, 105, 11613-11618.
- J. A. Champion and S. Mitragotri, *Proc. Natl. Acad. Sci.*, 2006, 103, 4930-4934.
- D. Dendukuri, D. C. Pregibon, J. Collins, T. A. Hatton and P. S. Doyle, *Nat. Mater.*, 2006, 5, 365-369.

11. S. H. Im, U. Jeong and Y. Xia, *Nat. Mater.*, 2005, 4, 671-675.
12. W. Wang, M.-J. Zhang, R. Xie, X.-J. Ju, C. Yang, C.-L. Mou, D. A. Weitz and L.-Y. Chu, *Angew. Chem. Int. Ed.*, 2013, 52, 8084-8087.
13. S. Xu, Z. Nie, M. Seo, P. Lewis, E. Kumacheva, H. A. Stone, P. Garstecki, D. B. Weibel, I. Gitlin and G. M. Whitesides, *Angew. Chem.*, 2005, 117, 734-738.
14. Y.-d. Yin and Y.-n. Xia, *Adv. Mater.*, 2001, 13, 267-271.
15. S. Sacanna, M. Korpics, K. Rodriguez, L. Colón-Meléndez, S.-H. Kim, D. J. Pine and G.-R. Yi, *Nat. Commun.*, 2013, 4, 1688.
16. J.-W. Kim, R. J. Larsen and D. A. Weitz, *J. Am. Chem. Soc.*, 2006, 128, 14374-14377.
17. J. P. Rolland, B. W. Maynor, L. E. Euliss, A. E. Exner, G. M. Denison and J. M. DeSimone, *J. Am. Chem. Soc.*, 2005, 127, 10096-10100.
18. J. A. Champion, Y. K. Katare and S. Mitragotri, *Proc. Natl. Acad. Sci.*, 2007, 104, 11901-11904.
19. P. Kolhar and S. Mitragotri, *Adv. Funct. Mater.*, 2012, 22, 3759-3764.
20. N. Doshi, J. N. Orje, B. Molins, J. W. Smith, S. Mitragotri and Z. M. Ruggeri, *Adv. Mater.*, 2012, 24, 3864-3869.
21. S. G. Jang, D. J. Audus, D. Klinger, D. V. Krogstad, B. J. Kim, A. Cameron, S.-W. Kim, K. T. Delaney, S.-M. Hur, K. L. Killops, G. H. Fredrickson, E. J. Kramer and C. J. Hawker, *J. Am. Chem. Soc.*, 2013, 135, 6649-6657.
22. K. Kataoka, A. Harada and Y. Nagasaki, *Adv. Drug Delivery Rev.*, 2012, 64, 37-48.
23. H. Zhang, J. Bei and S. Wang, *Biomaterials*, 2009, 30, 100-107.
24. R. Gref, Y. Minamitake, M. T. Peracchia, V. Trubetsky, V. Torchilin and R. Langer, *Science*, 1994, 263, 1600-1603.
25. J.-B. Fan, Y. Song, S. Wang, L. Jiang, M.-Q. Zhu and X. Guo, *RSC Adv.*, 2014, 4, 629-633.
26. T. Musumeci, C. A. Ventura, I. Giannone, B. Ruozi, L. Montenegro, R. Pignatello and G. Puglisi, *Int. J. Pharm.*, 2006, 325, 172-179.
27. B. Magenheim, M. Levy and S. Benita, *Int. J. Pharm.*, 1993, 94, 115-123.